



Journal of Applied Sciences

ISSN 1812-5654

science
alert

ANSI*net*
an open access publisher
<http://ansinet.com>

CFD Simulations of the 3D Velocity Profile of Paddle Agitator and Two-blade Impeller in Stirred Vessel with a Highly Viscous Newtonian Fluid

M. Bouzit, L. Benali, M. Hachemi and F. Bouzit
Department of Mechanics, University of Sciences and Technology of Oran,
USTO, BP1505EL M'Nouar, Oran, Algeria

Abstract: Computational Fluid Dynamics is used to solve 3D hydrodynamics of a mixing vessel for paddle agitators and two-blade impellers with different blade heights operating in laminar regime. These results are compared with available experimental data: good agreement is observed. The tangential velocities calculation was carried out for paddle agitator with height $W = 1.5T$. Early studies confirmed that this type of geometry generates essentially a tangential flow. The results obtained show good agreement with those obtained by many authors. The second agitator height was $W = 0.25T$ which behaves, generally, like a turbine and generates more important axial and radial velocities which are at the origin of secondary flows on both sides of the blade. The axial velocities calculation for blades of various heights confirmed the observations of many authors; especially, a maximum velocity for the lowest height considered. The position of the impeller in the tank was analysed and the axial velocity change with the positions of the impeller.

Key words: Laminar mixing, 3D modelling, Newtonian fluid, stirred vessel

INTRODUCTION

The knowledge of the distribution velocities in an agitated vessel proves to be primordial for the optimum dimensioning of the vessel and the agitator. The mixture of liquids using mechanical agitators is an operation largely used in chemical fields, cosmetic, pharmaceutical and agro- alimentary. Generally, the objective of the mixture is the homogenisation. An ideal mixture is a mixture, which produces a homogeneous mixture and allows an optimum time and cost. This early allow to determine some global parameters such as the time of mixture, the coefficients of thermal transfer as well as the power consumption which is the most important parameter in the processes of agitation. Currently, satisfactory methods are available. They permit the correct estimation of these agitation power valid for Newtonian liquids and non Newtonians one Ulbrecht *et al.* (1985) and Tatterson (1991). A larger diameter of paddle increases the power consumption on the one hand and increases the effectiveness of the agitation process on the other hand. The operation requires finding a compromise for the necessity of a better agitator dimensioning.

In practice, the liquids used in the processes of agitation are, highly viscous and consequently, have quite long times of mixture and also a quite important power consumptions. The combination of all these parameters gives a precise idea on the effectiveness of the mixture operation. The optimum dimensioning of the mixer

is conditioned by ability to evaluate and predict the performances of the agitator for various geometries and boundary conditions in relation to the aptitude to produce a homogeneous mixture. These performances are evaluated if the model of flow, which is developed in the mixer for particular conditions, is known. The performance of mixer can be evaluated if we know the flow pattern developed in the mixer under specific conditions. The objective of this study is especially to carry out an investigation by means of a computer three-dimensional calculation code in order to anticipate correctly the velocity field of a fluid in an agitated vessel provided with paddle agitator and two-blade impeller type while varying the geometry of the rotor. It should be noted that this type of code plays a very important part in the comprehension of the flows in the agitated vessel. It became a very useful tool for the very complex flows of the agitated fluids. The numerical simulation and the experimental validation allow improving the conception of many systems with engine. Part of the numerical results is compared with experimental results based on the same geometries. In addition, the study was limited to the regime with low Reynolds numbers, which appear in the majority of the practical applications.

GEOMETRY OF THE AGITATION SYSTEM

The simulated geometry (Fig. 1) consists of a cylindrical tank with a flat bottom; the liquid level H is equal to $1.5T$. The impeller consists of two vertical plane

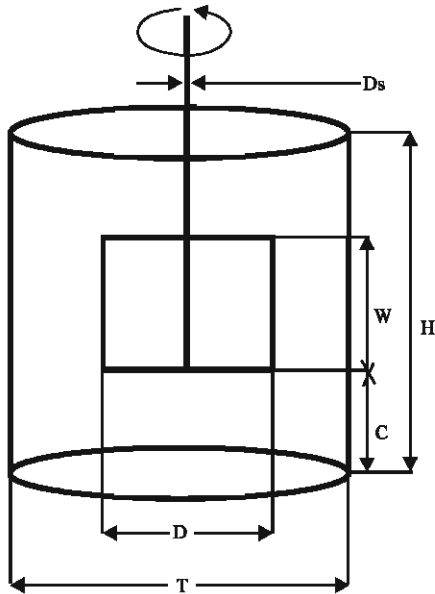


Fig. 1: Agitated system simulated

blades fixed on a cylindrical shaft. This impeller is placed in order to not scrape the bottom of the tank. The various geometries used are shown in table below.

W/T	1.50	0.25	0.25	0.25	0.25	0.25
H/T	1.50	1.50	1.50	1.50	1.50	1.50
D/T	0.50	0.50	0.50	0.50	0.50	0.50
Ds/T	0.046	0.046	0.046	0.046	0.046	0.046
C/T	0.066	0.066	0.133	0.266	0.533	0.625

THEORETICAL CONSIDERATIONS

The rotation of the impeller introduces a periodic hydrodynamic mode. To obtain a steady flow and to simplify the writing of the boundary conditions, we chose a rotating frame. The boundary conditions consist of setting each velocity component equal to zero on the blades, because of the rotating frame and setting the angular velocity component equal to the rotation velocity at the vertical walls of the tank. The theoretical developments of the field velocity are presented in some of articles Hiraoka and Yamada (1978), Abid *et al.* (1994) and Yu *et al.* (2005). All results are presented in dimension less values, which enable the user to investigate any size of vessels.

NUMERICAL SIMULATION

The numerical simulation used in this study using a CFX5.7 code for which the resolution of the Navier-stokes

equations governing the phenomena of transfer of momentum are solved by a finite volumes method. The grid used is tetrahedral, the number of elements and nodes varies from geometry to another: (202000 to 387000) elements and of (62000 to 120000) nodes. In each simulation, the solution is considered convergent when the residues of the three components velocity are lower than 10^{-5} . CPU time varies between 930 and 2580 sec.

PADDLE AGITATOR

Figure 2 and 3 give the profiles of the dimension less tangential velocity component ($V_{\theta}/\pi ND$) for Reynolds number of 4 at $Z^* = 0.87$ in the vessel are compared with profiles from Bertrand (1983) and from Youcefi (1993) obtained with hot film probe rotating with the agitator.

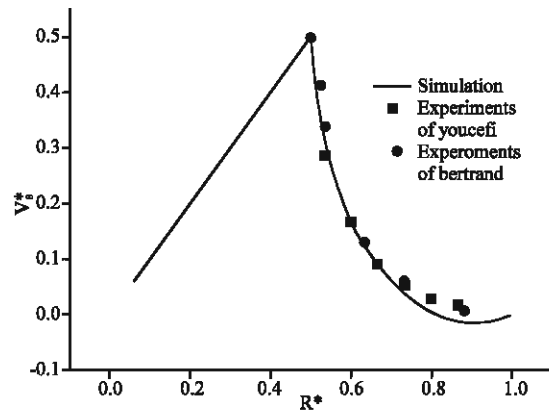


Fig. 2: Tangential velocity component ($W/T = 1.5$) $\theta = 0^\circ$, $Re = 4$, $Z^* = 0.87$

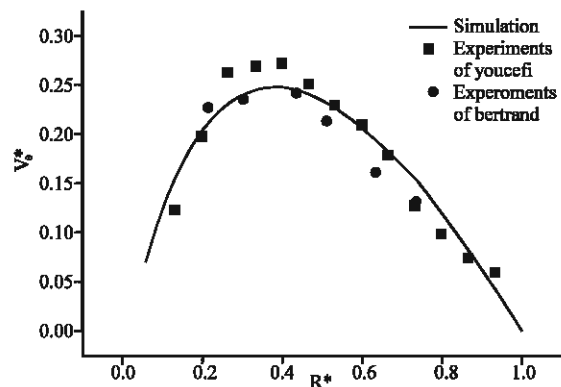


Fig. 3: Tangential velocity component ($W/T = 1.5$), $\theta = 90^\circ$, $Re = 4$, $Z^* = 0.87$

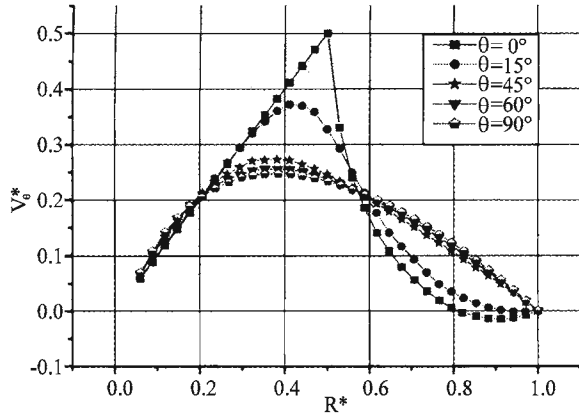


Fig. 4: Tangential velocity component ($W/T = 1.5$), $Re = 4$, $Z^* = 0.87$

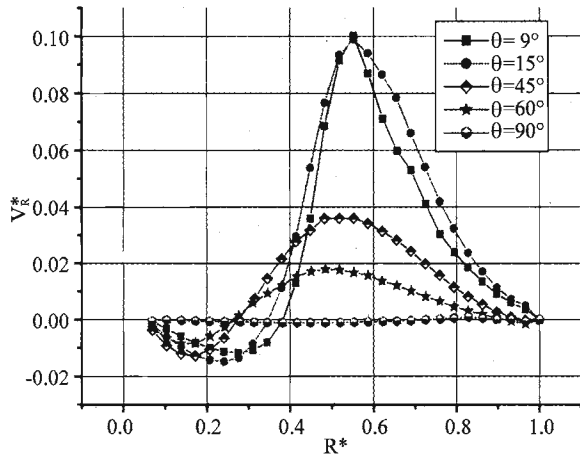


Fig. 5: Radial velocity component ($W/T = 1.5$), $Re = 4$, $Z^* = 0.87$

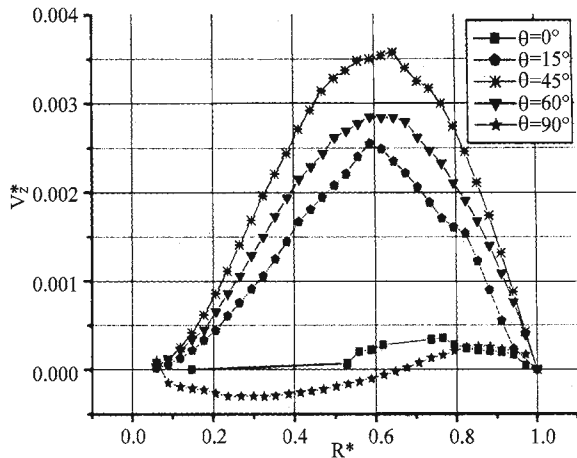


Fig. 6: Axial velocity component ($W/T = 1.5$), $Re = 4$, $Z^* = 0.87$

For same conditions as above, Fig. 4 gives the distribution for tangential velocity for various angles. It also shows that the maximum value of the tangential velocity is always located at the impeller tip as given by authors Youcefi *et al.* (1997), Anne-Archard and Boisson (1995) and Bertrand and Couderc (1982). and it decrease from about 50% between 0° and 90° (Bouzit *et al.*, 2004).

The profiles of the dimension less radial velocity component ($V_R/\pi ND$) at the same height and angular positions are presented in Fig. 5. The maximum values of radial velocity are obtained for the impeller tip and for angular positions between 9° and 15° . It can be noted that the radial velocity components are negative close the surface of the impeller.

Figure 6 gives the distribution of dimension less axial velocity for various angles between $\theta = 0^\circ$ (the impeller) and $\theta = 90^\circ$. We notice that the axial velocity is maximum for $R^* = 0.6$ and for an angle of approximately 45° . It can be noted that for paddle agitator ($W = 1.5 T$) the axial velocity component is not to be taken into account and the flow generated by this kind of impeller is essentially tangential

TWO-BLADE IMPELLER

In this part, The flow produced by a two-blade impeller is considered (Fig. 7).

The ratio between the impeller diameter and the blade height is ($W/T = 0.25$). The impeller is located at mid-height of the tank ($C/T = 0.625$). The ratio between the tank diameter and the impeller diameter is ($D/T = 0.5$).

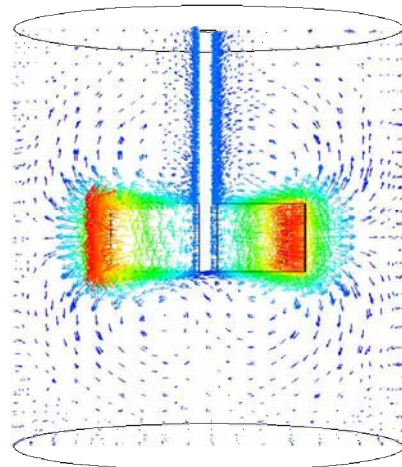


Fig. 7: (plan $\theta = 0^\circ$)

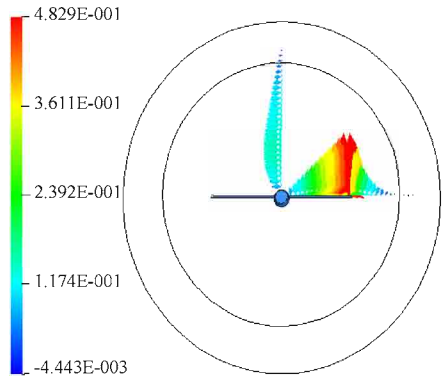


Fig. 8: Tangential velocity component ($W/T = 0.25$), $Z^* = 0.75$

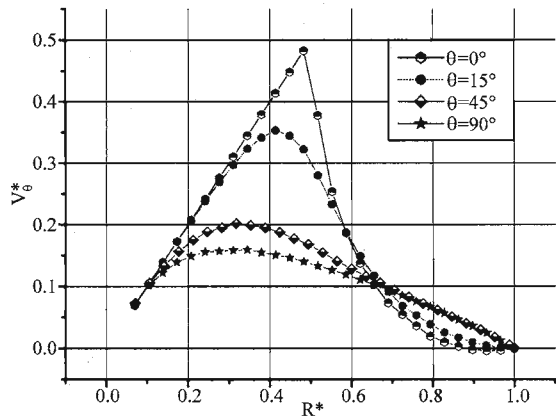


Fig. 9: Tangential velocity component ($W/T = 0.25$), $Re = 20$, $Z = 0.75$

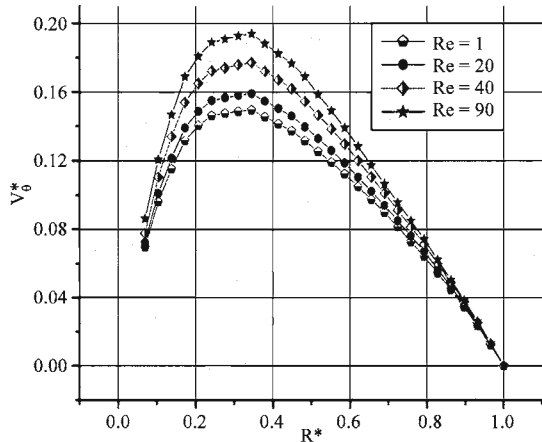


Fig. 10: Tangential velocity component ($W/T = 1.5$), $\theta = 90^\circ$, $Re = 4$, $Z^* = 0.87$

Figures 8 and 9 shows the field of tangential velocity on the level of the blade and its prolongation ($\theta = 0^\circ$) and on $\theta = 90^\circ$ (Fig. 10) which was obtained for $z^* = 0.75$

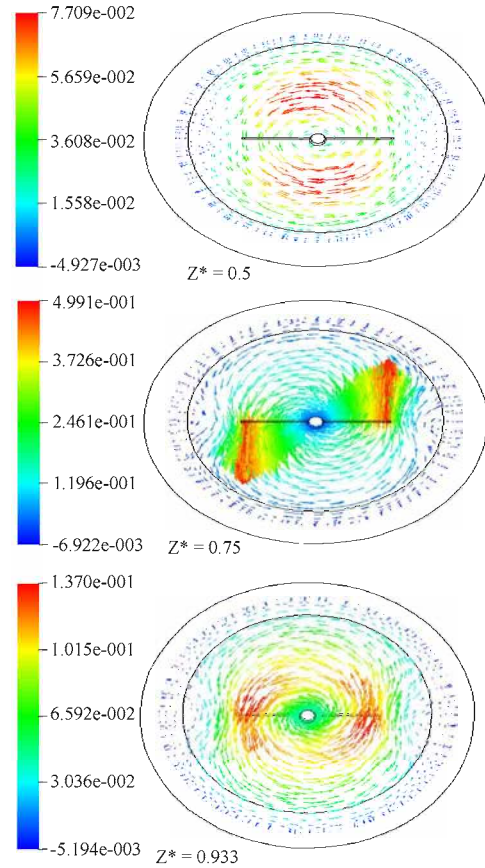


Fig. 11: Tangential velocity component ($W/T = 0.25$), $Re = 20$

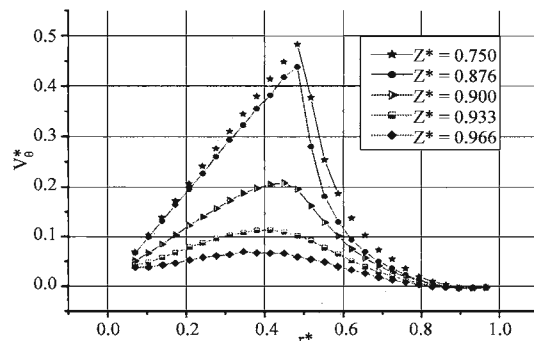


Fig. 12: Tangential velocity component ($W/T = 0.25$), $\theta = 0^\circ$, $Re = 20$

(mid-height of impeller). As the W/T ratio becomes smaller, the two blade impeller becomes turbine. This geometry generates more important axial velocities. We can easily see that the flows are directed to the axes in a spiral. The formation of recirculation in top and in low of the blade. These results were observed by other authors.

Measures taken with various heights give the tangential velocity component. Fig. 11 shows that for the

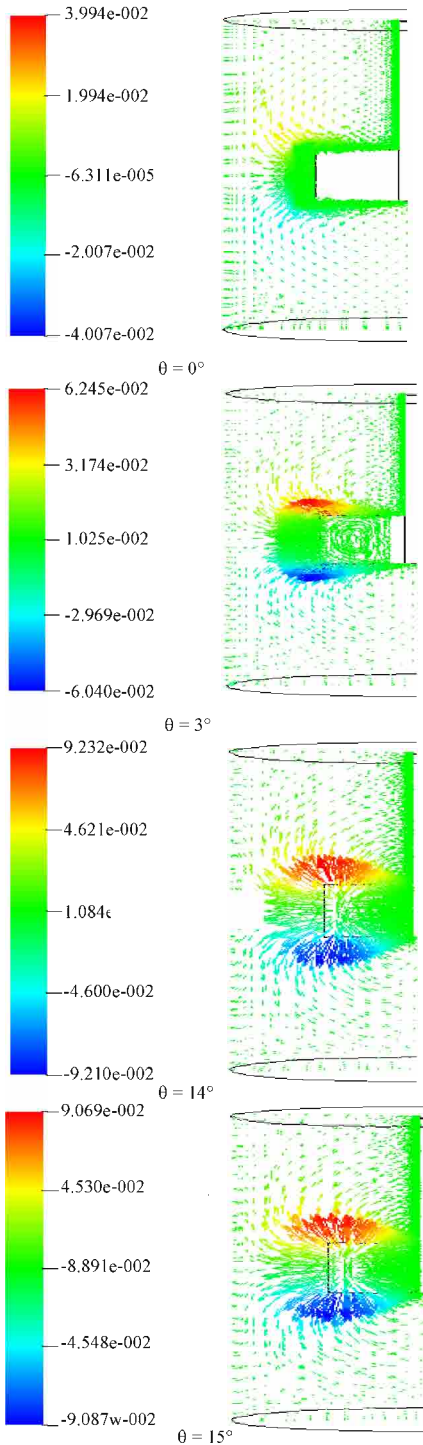


Fig. 13: Axial velocity component

flow in horizontal planes the maximum tangential velocity is located at the end of the blades and it is more important in the plan $z^* = 0.75$ (mid-height of the blade).

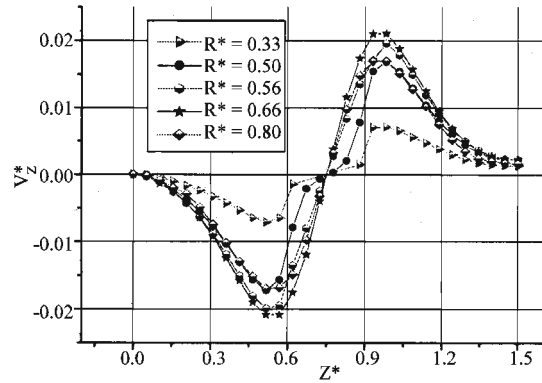


Fig. 14: Axial velocity component ($W/T = 0.25$), $Re = 20$, $\theta = 0^\circ$

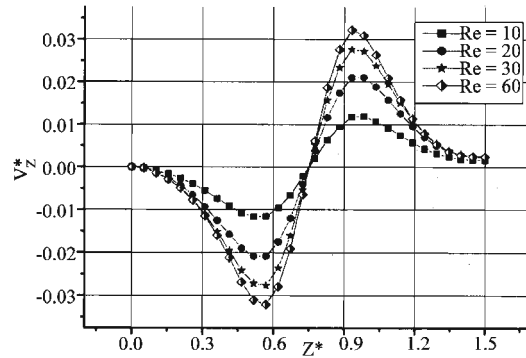


Fig. 15: Axial velocity component ($W/T = 0.25$), $R^* = 0.666$, $\theta = 0^\circ$

Figure 12 represent the distribution of the tangential velocities on the blade and its prolongation for various heights. The results obtained show that the maximum tangential velocity is located at the mid-height of the blade and the move away towards the bottom of the tank and towards the free face this velocity decrease. Identical results were found by Kuncewicz and Pietrzykowski (2001).

The axial velocity components (Fig. 13) generated by two blade impeller ($W/T = 0.25$) positioned in the mid-height of the tank are given for $Re = 20$ and various angles resulted from Fig. 14 reveal maximum velocities at the higher and lower edge of the blade for an angle of approximately of 14° , which confirms the existence of two vortices on both sides of the blade.

The axial velocity component was given for the same conditions as above for various vertical planes. The curves obtained and represented in Fig. 14 give, for the various plans, a null velocity on the mi-height of the blade. On the other hand, axial velocities on the higher edge and the lower edge of the blade are maximum and of opposite direction. These results largely comfort those obtained previously. We can notice, also, that axial velocities are higher in the plan $R^* = 0.666$. The last three

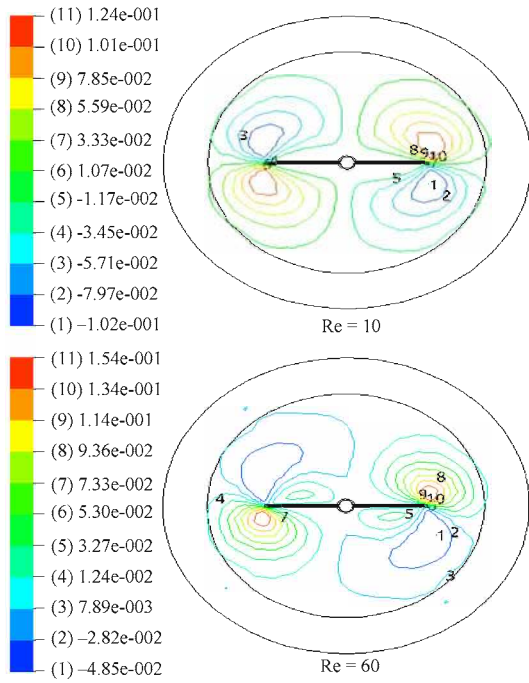


Fig. 16: Contour of radial velocity component

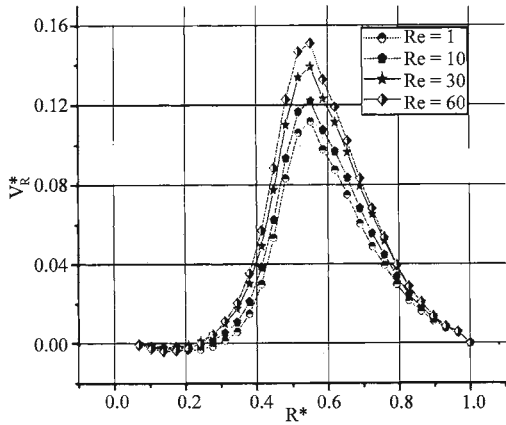


Fig. 17: Radial velocity component ($W/T = 0.25$), $\theta = 10^\circ$

results gives a maximum axial velocity in angular position of 14° and in the vertical plane $R^* = 0.666$.

The distribution of dimension less axial velocities in the plan $R^* = 0.666$ was given for various Reynolds numbers. The shape of the curves of distribution of Fig. 15 is identical to that obtained previously. Obviously, the intensity axial speeds is directly proportional to the Reynolds number.

The contour of the radial velocity components generated by the two blade impeller ($W/T = 0.25$), $\theta = 10^\circ$ represented in Fig. 16 for various Reynolds numbers. Radial maximum velocities are located at the two ends of

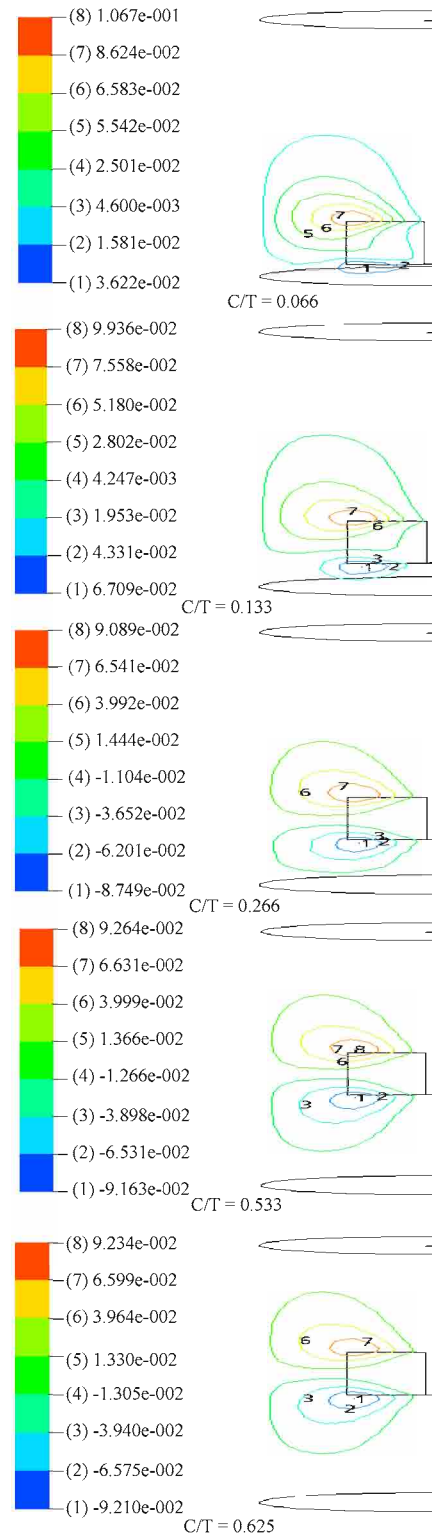


Fig. 18: Axial velocity component ($W/T = 0.25$), $\theta = 0^\circ$

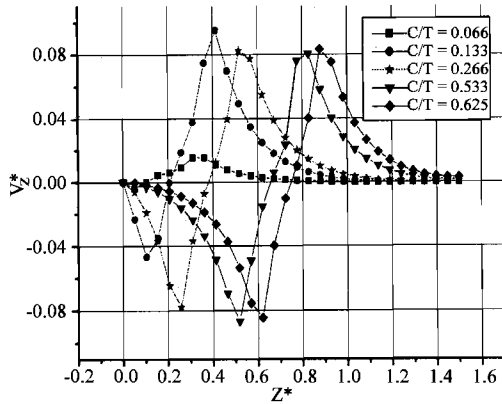


Fig. 19: Axial velocity component ($W/T = 0.25$), $Re = 20$, $\theta = 14^\circ$, $R^* = 0.5$

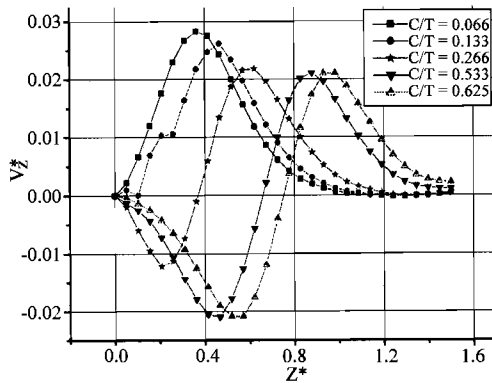


Fig. 20: Axial velocity component ($W/T = 0.25$), $Re = 20$, $\theta = 0^\circ$, $R^* = 0.66$

the blade. This is explained by the fact why centrifugal force has tends to accelerate the fluid in the direction of the wall of the tank; whereas the latter tends to slow down it. We can, also, notice a zone of over pressure upstream of the blade and a trough of low pressure downstream. The maximum values of the radial velocity are obtained at close to $\theta = 10^\circ$. The increase in the Reynolds number increases the intensity of radial velocity appreciably (Fig. 17).

Figure 18 gives the influence of the position of the impeller in the tank in the axial flow. Figure 19 shows that at $\theta = 14^\circ$ and $R^* = 0.5$ in the lower part of the blade more we move away from the bottom axial velocity increases. Fig. 20 shows the influence of bottom on the axial flow in the axe of the impeller. When we move away from the bottom, the axial velocity decrease in the higher part of the impeller and increase in the lower part of the impeller.

CONCLUSIONS

The study carried out and presented in this present paper relates to the evaluation and determination of the fields velocities for agitators of various geometries and

the evaluation of this agitator on the effectiveness of agitation. The results obtained reveal some known behaviours, but the originality of this work is especially to try to quantify the required components and to give with more exactitude the points where the values of these components are maximum or minimal and the influence of the position of the impeller in the axial flow. We can note, a distribution of tangential velocities on the blade and his prolongation presenting a peak at the tip of the blade. This profile speeds subsides with the increase in the angles, until it becomes parabolic form at $\theta = 90^\circ$. The reduction height of the blade has a considerable effect on the increase axial velocity. This type of geometries which is compared to a turbine often generates secondary flows on both sides of the blade. Hiraoka *et al.* (1978) showed, also that the height of the blade plays a major part in the birth of these secondary flows. This type of flow contributes partly to the effectiveness of the process of agitation. However, it should well be noted that the turbines of low heights are at the origin of dead zones located at the bottom of the tank and close to the free surface.

NOMENCLATURE

- C = distance between tank bottom and impeller (m)
- D = agitator diameter (m)
- Ds = shaft diameter (m)
- H = liquid level (m)
- N = rotational speed of impeller (s^{-1})
- R = radial coordinate (m)
- R^* = dimension less radial coordinate ($2R/T$)
- Re = Reynolds number ($\rho ND^2/\mu$) (-)
- T = tank diameter (m)
- V_r = radial velocity component ($m \text{ sec}^{-1}$)
- V_r^* = dimension less radial velocity ($V_r/\pi ND$)
- V_z = axial velocity component ($m \text{ sec}^{-1}$)
- V_z^* = dimension less axial velocity ($V_z/\pi ND$)
- V_θ = tangential velocity component ($m \text{ sec}^{-1}$)
- V_θ^* = dimension less tangential velocity ($V_\theta/\pi ND$)
- W = agitator height (m)
- Z = axial coordinate (m)
- Z^* = dimension less axial coordinate (Z/T)
- θ = tangential coordinate, angle
- μ = viscosity of the liquid ($kg.m^{-1}.s^{-1}$)
- ρ = density of the liquid ($kg.m^{-3}$)

REFERENCES

- Abid, M., C. Xuereb and J. Bertrand, 1994. Modeling of the 3-D Hydrodynamics of 2-Blade impellers in stirred tanks filled with a highly viscous fluid. *Can. J. Chem. Eng.*, 75: 184-193.

- Anne-Archard, D. and H.C. Boisson, 1995. A finite element simulation of the crossed-effects of viscoelasticity and inertia in an agitated vessel. *Intl. Num. Meth. Fluids*, 21: 75-90.
- Bertrand, J. and J.P. Couderc, 1982. Agitation de Fluides Pseudoplastiques par un Agitateur Bipale. *Can. J. Chem. Eng.*, 60: 738-747.
- Bertrand, J., 1983. Agitation de fluides visqueux: Cas de mobiles à pales, d'ancres et de barrières. Thesis Ph.D INP Toulouse, France.
- Bouzit, M., M. Hachemi, M. Abidat and A. Youcefi, 2004. Simulation numérique de l'écoulement de fluides incompressibles inélastiques dans une cuve mécaniquement agitée par un agitateur bipale. 2eme Colloque International de Rhéologie (Ghardaia) 09-12 Décembre 2004.
- Hiraoka, S. and I. Yamada, 1978. Numerical analysis of flow behaviour of highly viscous fluid in agitated vessel. *J. Chem. Eng. Japan*, 11: 487-493 .
- Kuncewicz, Cz. and M. Pietrzykowski, 2001. Hydrodynamic model of a mixing vessel with pitched-blade turbines. *Chem. Eng. Sci.*, 56: 4659-4672.
- Tatterson, G.B., 1991. Fluid Mixing and Gas Dispersion in Agitated Tanks. McGraw-Hill, New York.
- Ulbrecht, J.J. and P.J. Carreau, 1985. Mixing of Viscous Non-newtonian Liquids. In: *Mixing of Liquids by Mechanical Agitation*. Ulbrecht, J.J. and G.K. Patterson, (Eds.). Chapter 4, Gordon and Beach, New York,
- Youcefi, A. , 1993. Etude Expérimentale de l'Écoulement d'un Fluide Viscoélastique autour d'un Agitateur Bipale en Cuve Agitée. Thèse de Doctorat, INP de Toulouse, France.
- Youcefi, A., D. Anne-Archard, H.C. Boisson and M. Sengelin, 1997. On the influence of liquid elasticity on mixing in a vessel by a two-bladed impeller. *J. Fluids Eng. (Trans. ASME)*, 119: 616-622.
- Yu, C. and S. Gunasekaran, 2005. Performance evaluation of different model mixers by numerical simulation. *J. Food Eng.*, 71: 295-303.